Supplementary Information—Analytical Instrumentation

S-1. Pre-Basic Characterization (Pre-BC) Instrumentation

S-1.1 Magnetometer and magnetic susceptibility

A **Magnetometer** is an instrument used to measure magnetic forces. **Magnetic susceptibility** is a measure of how much a material becomes magnetized in an applied magnetic field. Combining these two complementary measurements enables an estimation of the ancient martian field strength that magnetized the samples, monitors the possibility of magnetic alteration of the samples and provides information about the magnetic mineralogy. These measurements can be a baseline to monitor for the possibility of magnetic contamination of the samples while in storage. We note here that the sample tubes will not have experienced magnetic fields higher than 0.5 mT from collection through Earth return as required by MSR. Spinner magnetometers (Figure S-1a) do not have many mechanical components and chemical compounds (gear, cam, slider, electric motor, metal ball bearings, oils, etc.) unlike SQUID instruments that cannot be used to avoid chemical contamination and can accommodate larger samples > 10 cm^3 (about 30 g) (Nagendran et al., 2011). The samples are enclosed in a cube made of transparent acrylic resin (PMMA) plates welded by solvents. Cubes with different dimensions (5, 7, 10, 12, 15, 17, and 20 cm sides) were used to best fit various sample sizes and shapes. Samples are kept tight in the cubes using Teflon films and/or PMMA rings (Figure S-1a-c).

Constraining the origin of the magnetic fields on Mars is a science priority of this mission and this measurement needs to be done prior to the sample being removed from the tube to make sure there is no disturbance to the paleomagnetic orientations and so we are minimizing subsequent contamination by viscous remagnetization once they arrive in Earth's magnetic field. These measurements need to be completed again before the samples are allocated. Magnetic susceptibility is strongly controlled by lithology (Lepaulard, 2019) and therefore sedimentary rocks could be considered the priority for these measurements. These measurements are fast, non-destructive, and non-contaminating and can be automated.

S-1.2 X-ray computed tomography (XCT) scanner

We have identified some compelling reasons to perform penetrative 3D imaging prior to opening the sample tubes. Some examples identified are the following: 1) Samples that record paleomagnetic orientations; 2) Samples that have finely stratified sedimentary rocks (where the relationship of the layers in relation to each other are important to document); 3) Samples where documentation of high-value veins, fluid inclusions or other special geometric attributes are needed for subsequent sampling or for the sample catalog, 4) Porosity and density measurements. Therefore, there needs to be at least one penetrative imaging technique to characterize the samples while still in the sample tube. Three major penetrative imaging techniques were discussed, which are 3D synchrotron X-ray computed microtomography (XRCMT), neutron computed tomography (NCT) and laboratory-based 3D high resolution X-ray computed microtomography (XCT). See section S-5 for discussion for why NCT and XRCMT were ruled out.

***Figure S-1a**. left. Schematic illustrations of the magnetometer in the top view opening the top cover (a) and the side view showing the interior by a broken-out section of the shield (S-1b). A two-layered mu-metal shield (1) enclosing a three-axis fluxgate sensor (7) mounted on a sensor holder (8) that can slide on a rail (3), and a sample (4) on a rotating table (5). The sensor-to-sample distance is adjusted by changing the position of the pin (9) fixed on bores (10). The user can rotate the table by a handle (14) and the rotation angle is measured by an optical encoder unit (13). The power supply and the outputs of the sensor are connected to the outer signal conditioning unit via feedthrough (2) and a connector (12). The mu-metal shield and the entire system is mounted on an aluminum plate (6) supported by aluminum feet (11). The coordinate system is shown in the figures. The horizontal and vertical lines in (**S-1b**). show rotation axis and the horizontal centerline of the sensor, respectively (Uehara et al., 2017) (**S-1c**) Three-axis fluxgate magnetic field sensor (Mag-03MS100, Bartington Instruments, Ltd.*) and a rotating sample stage with two-layer mu-metal magnetic shield (550 mm in diameter and 500 mm in height) (photo credit: Professor Ben Weiss). *The naming of this reference instrument is intended for planning and discussion purposes only. Instrument-level performance requirements, sufficient to conduct a competitive procurement, have yet to be written.*

X-ray Computed Tomography is a largely non-destructive method of analyzing extraterrestrial samples at the micrometer-level scale (Zeigler et al., 2021). High resolution XCT illuminates the sample with X-ray photons, which interact principally with electrons in the sample, so contrast in XCT images is generated by local differences in chemistry and correlates roughly with mean atomic weight, although density and other factors also affect X-ray attenuation coefficients. Significant data on the internal texture of a material may be collected without (or before) the portioning of the sample and these measurements can be done on-site at the Sample Receiving Facility, eliminating the need to transport samples off-site. The versatility of XCT stems from its sensitivity to sample properties (density, composition) that commonly show variation in extraterrestrial samples (Carlson, 2006). For example, these measurements are ideal when samples need to be subsampled or allocated in specific lithologies (e.g., basalts or impact-melt breccias) for detailed analyses and targeted investigations (McCubbin et al., 2021 and other efforts related to the ANGSA Program, Figure S-2a). Another example where these measurements are helpful is when fractures, veins, porosity, lithologic and possibly mineralogical-based heterogeneities need to be identified (Welzenbach et al., 2018). The voxel resolution for any instrument is a function of both the geometry of the XCT system and the geometry of the sample itself (Hanna and Ketcham, 2017).

Consequently, the instrument that is selected for the SRF should be optimized to attain the highest voxel resolution that can be achieved on the sample tubes. It may be possible to conduct XCT on the sample tubes while they are inside the STIC, which would reduce the time the sample tube spends outside of an isolated environment, and this option should be considered as the STIC design is optimized (see Section 8.1, Future Work 8). For example, we were able to use helical scanning to double the voxel resolution for the Apollo Drive Tube 73002 relative to a conventional XCT scan. A future group can determine the minimum voxel resolution requirement for the Mars samples once we know a little more about the samples that would be returned; however, the instrument selected should be able to scan the length of the tube in its entirety (Z-direction, ca. 14 cm) in one scan without stitching images together.

Although XCT is generally considered to be a non-destructive technique since inorganic materials are not affected by X-ray exposure, there are concerns that these measurements can be detrimental to organics in these samples, however preliminary results are promising that organics are minimally affected if at all at high X-ray energies (Friedrich et al., 2016; 2018; Hanna and Ketcham 2017). There have also been studies on how ionizing radiation impacts thermoluminescence data (Sears et al., 2016). Given that this technique would be used as part of pre-BC and could be applied to entire sample tubes, substantial research efforts to evaluate the effects of XCT on samples is warranted and should be supported in the coming years, especially on labile organics like DNA etc. from extant life. Lab XCT instruments are reliable and do not typically exhibit a lot of downtime, so only one instrument may be required for the SRF, but a future group tasked with optimizing budget and schedule should evaluate the number of XCT instruments required in the SRF (See Section 8.1, Future Work 9).

FINDING C-8: There are compelling reasons to perform penetrative 3D imaging prior to opening the sample tubes. A laboratory-based X-ray Computed Tomography scanner is the best technique to use and the least damaging to organics of the penetrative imaging options considered.

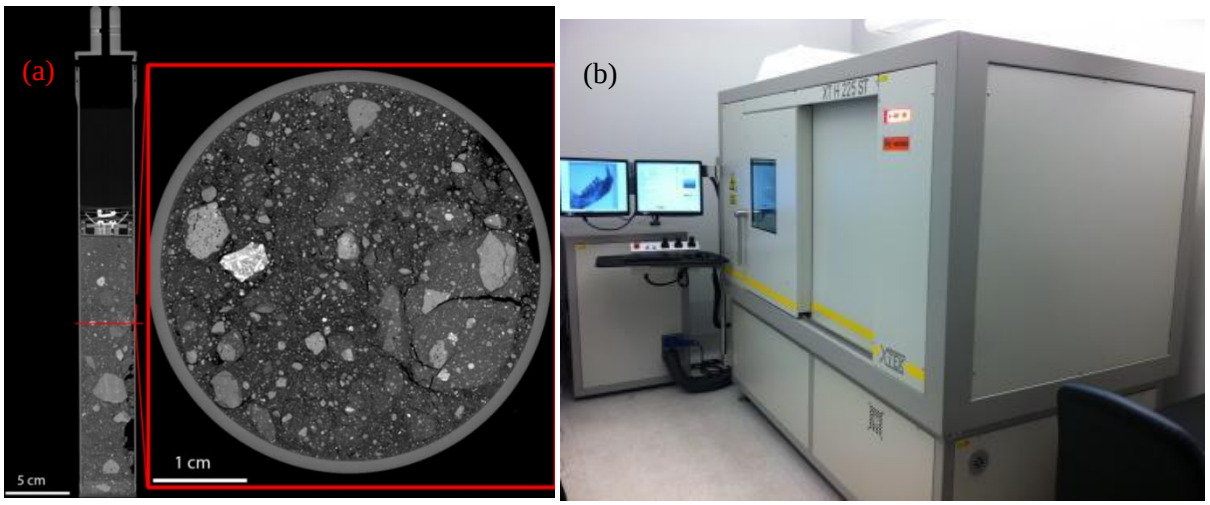

Figure S-2a *(left). X-ray Computed Tomography image of Apollo Drive Tube 73002 (Zeigler et al., 2021);* ***S-2b****. Example of XCT instrument Nikon XTH 225 ST* with a 225 kV rotating source. Pictured Duke University, Engineering Department, (L x W x H) 2.4 m x 1.3 m x 2.2 m and it weighs 4,200 kg. *The naming of this reference instrument is intended for planning and discussion purposes only. Instrument-level performance requirements, sufficient to conduct a competitive procurement, have yet to be written.*

S-2. Basic Characterization Instrumentation

S-2.1 Analytical balance

A high precision laboratory analytical balance is used for measuring mass, typically designed with an enclosed measuring pan to avoid the influences of dust and air currents (Figure S-3). These measurements are used for accurate curatorial records and documentation, and for inclusion in the sample catalog. This is typically a quick measurement, non-destructive and non-contaminating and done within the isolator. We do not foresee any need to disaggregate material, just weigh as is when removed from the sample tube. An analytical balance measures the mass of the sample to 0.0001 g (or greater) and is extremely accurate. The environment of the lab, operating temperature, humidity, vibration, and ventilation currents can all affect performance. Consequently, it is important to keep the balance inside an enclosed space, keep it clean, make sure it is leveled correctly, and make sure it is regularly maintained and serviced.

***Figure S-3**. Example of an analytical balance, VWR T-Series Balances* (W × D × H) approximately 206 × 333 × 355 mm, weight: <11 kg.*

** The naming of this reference instrument is intended for planning and discussion purposes only. Instrument-level performance requirements, sufficient to conduct a competitive procurement, have yet to be written.*

Lesson Learned, Analytical Balance: Commercially available balances include plastics and metals (like gold and lead) and do not meet materials requirements for use inside a pristine isolator. Analytical balances used in existing curation facilities, like JSC are heavily modified to meet materials requirements. When the pristine isolator requirements are set for the BSL-4 facility in the future, this needs to be considered for all analytical instruments that might be used inside the pristine isolator.

S-2.2 Binocular stereo light microscope (with camera and video capabilities)

A binocular stereo visible light microscope is required (Table 1, goals 2 and 3) for the visual investigation of the surface of the sample to reveal surficial physical characteristics and assess degree of sample heterogeneity e.g., color, grain size and shape, textural relationships (Figure S-4). This microscope needs to have the ability to take photography and live video streaming to allow filming but also remote access for live observation and should have at least 8:1 zoom ratio, which is a standard zoom ratio on stereo microscopes. Using a visible light microscope is a fast, essentially non-destructive examination, does not contaminate the sample and no sample preparation is required. These examinations would be done within the isolator and would be a major tool to do a lot of the descriptions of the Basic Characterization phase. The spatial resolution is governed by the geometry of the setup, but likely mm to sub-mm resolution.

***Figure S-4**. Example of a Leica* binocular stereo light microscope attached to a glovebox.*

** The naming of this reference instrument is intended for planning and discussion purposes only. Instrument-level performance requirements, sufficient to conduct a competitive procurement, have yet to be written.*

S-2.3 *Multispectral imaging (400–1000 nm wavelength) and hyperspectral scanning (400–2500 nm)*

Multispectral imaging and hyperspectral scanning are spectroscopic reflectance techniques that are necessary (see Table 1, goals 2 and 3) to record chemical and mineralogical properties of the surface of the core samples, including sample heterogeneity and sample maturity (degree of sorting in sedimentary samples) in a wide range of wavelengths, greater than light from just the visible spectrum (400–700 nm). The large number of bands (typically hundreds) of hyperspectral sensors is used to expand our observations of the samples into the Visible to/and Near Infrared (VNIR) range to detect phenomena that are difficult or impossible to observe by eye. The spatial resolution is governed by the geometry of the setup, but likely mm to sub-mm resolution. Using multispectral and hyperspectral imaging is considered non-destructive to organic and inorganic materials (Sun et al., 2021) and does not contaminate the specimen. Given that the light source and spectrometers are mounted on the outside of the isolator or glovebox, these instruments can be shared among the various isolators/gloveboxes (Figure S-5a). Use of this technique requires a viewport through which the sample can be observed that can accommodate the geometry of the setup. It also requires using a viewport material that does not interfere with the spectral range of interest. For example**,** the borosilicate glass used in Apollo gloveboxes allows for the transmission of 400–2500 nm wavelengths without absorption features (Figure S-5b).

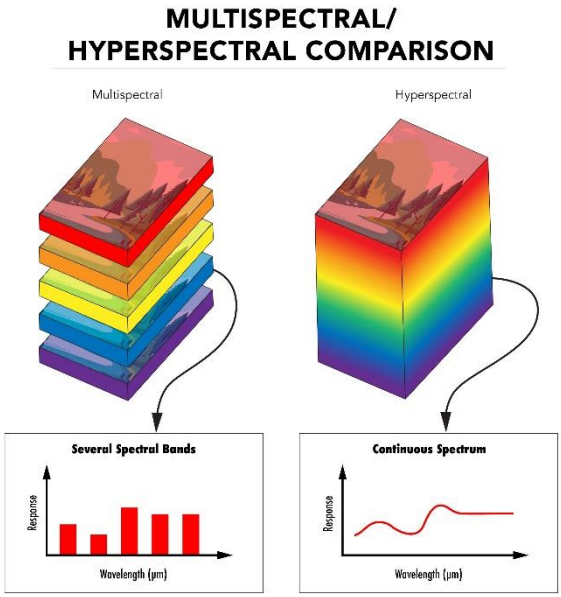

Figure S-5a *(left). Multispectral and hyperspectral measurements in a glovebox of Apollo samples for ANGSA at the Johnson Space Center. Photo credit: Juliane Gross.* ***S-5b*** *(right). multispectral and hyperspectral comparison from https://www.edmundoptics.fr/knowledge-center/application-notes/imaging/hyperspectral-and-multispectral-imaging/*

S-3. Preliminary Examination Instrumentation

S-3.1 Scanning Electron Microscope

A Scanning Electron Microscope (SEM) is a powerful tool commonly used in Earth and Planetary Science to make physical and chemical observations at the micrometer to nanometer level. A SEM scans a focused electron beam over a surface to create an image (e.g., Figure S-6). These same electrons interact with the sample, penetrating the sample surface by a couple of microns, producing various signals (secondary electrons, backscattered electrons, cathodoluminescence and characteristic X-rays) that can be used to obtain information about the surface topography and chemical composition. The resolution of a SEM depends on multiple factors, such as the electron spot size and interaction volume of the electron beam with the sample. Two different type of electron sources are used in SEMs - thermionic sources (tungsten filament, LaB_6 and CeB_6 cathodes) and field emission sources. Field emission SEMs (FE) offers some advantages over the more traditional SEMs using thermionic sources, with FE providing higher imaging resolution and longer source lifetimes.

With conventional SEMs, a sample is placed within a sample chamber and a high vacuum is applied (Figure S-7a,b). When the electron beam interacts with the sample there is a charge, which needs to be dissipated with carbon tape, or a thin layer of carbon or gold coating on the sample. Advances in technology now allows these instruments to operate at a variety of chamber pressures, with low pressure gas (up to several hundred Pa) or water vapour (up to several kPa) atmospheres, as well as standard high vacuum mode. This flexibility allows for the examination of unprepared samples i.e., samples that have not been coated with conductive material, or those samples which may be compromised by exposure to a high-vacuum environment, such as carbon-bearing samples and hydrated minerals. It is also possible to investigate samples which have been prepared for analyses, such as polished thin sections and polished

blocks. These versatile instruments are known as Variable Pressure (VP) or Environmental (E) SEMs. The environment in an VP-SEM can be water vapour, air, nitrogen, argon, and oxygen, and matching the environment that the sample has been under in the isolator would be ideal.

Characteristic X-ray photons are emitted when an outer shell electron populates the position (hole) of an inner electron that has been displaced by the instrument's electron beam. Each element has a unique energy difference between these shells. The energy of the X-rays that are emitted can be detected Energy Dispersive Spectrometer (EDS), which provides semi-quantitative chemical information and a quantitative elemental identification using a Wavelength Dispersive Spectrometer (WDS) from chemical elements with atomic numbers of 5 (boron) and higher. However, there are some limitations to this instrument - several geologically important elements cannot be measured with EDS and WDS, such as H, Li and Be and this instrument cannot distinguish among valence states of elements (e.g., Fe^{2+} and Fe^{3+}) nor distinct masses of an element (isotopes).

Modern SEMs typically have several ports for adding different detectors for imaging and analysis. To maximise the utility of the SEM in the SRF, a variety of detectors would be required - Back Scattered Electron Detector (BSE) and Secondary Electron Detector (SE) for imaging, Energy-dispersive X-ray Spectrometer (EDS/EDX) and Wavelength Dispersive Spectrometer (WDS) for measurements of chemical elements, Electron Back-Scatter Diffraction (EBSD) for crystallographic assessment and Cathodoluminescence (CL) detector for compositional and structural assessment.

SEMs with an ion source as well as an electron source are also now widely available. These Dual Beam Focused Ion Beam (DB FIB) sources are used to prepare small (micron scale) sub-samples for other techniques such as transmission electron microscopy. It should be considered to also include a FIB source in the SEM specification. An anti-vibration table or flooring to isolate the instrument from vibrations from the other instrumentation should be considered too.

The scanning electron microscope is a versatile and very powerful tool and the measurements it makes are made stronger combined with other PE tools, typically ones that measure crystal structure, such as the Confocal Raman Spectrometer or an X-ray Diffractometer.

It is strongly recommended that a VP-FE-SEM instrument(s) is available in the SRF to perform various sample measurements necessary for preliminary examination to meet the various requirements of the initial sample characterization (Table 1, goal 4). The absence of an electron microscope in the SRF would severely limit the ability to characterize the textures, mineralogy, and chemistry of the different samples to the level needed for allocations for sample safety analyses and time-sensitive science conducted within the SRF and for allocations to the wider scientific community. It could be advantageous to have more than one SEM within the SRF, for example having a dedicated instrument for sample tubes from the different caches, having instruments that are dedicated to organic-bearing samples and those that appear to be organic-poor or organic-free based on rover data. Having more than a single SEM is also highly advantageous in maximizing efficiency and minimizing delays or bottlenecks within the PE workflows, given the importance and utility of SEM investigations to inform decision-making on sample allocations.

It should be noted that electron and ion microscopy technologies are likely to advance dramatically over the next few years and we note that a Helium Ion Microscope is a new development and has great potential as an instrument as well.

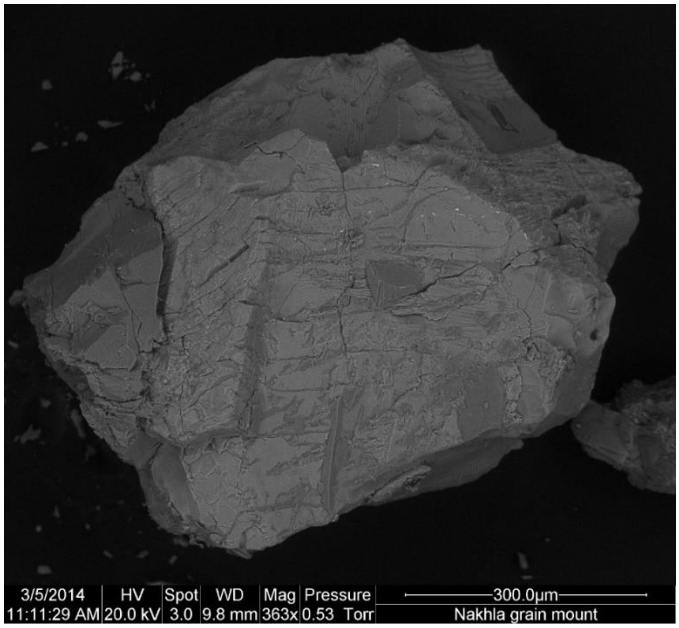

Figure S-6*. An uncoated and unprepared piece of a martian meteorite Nahkla (NHM London, accession number BM.1913,2.5) 363x magnification, 0.53 Torr pressure. Photo credit, M. R. Lee, University of Glasgow.*

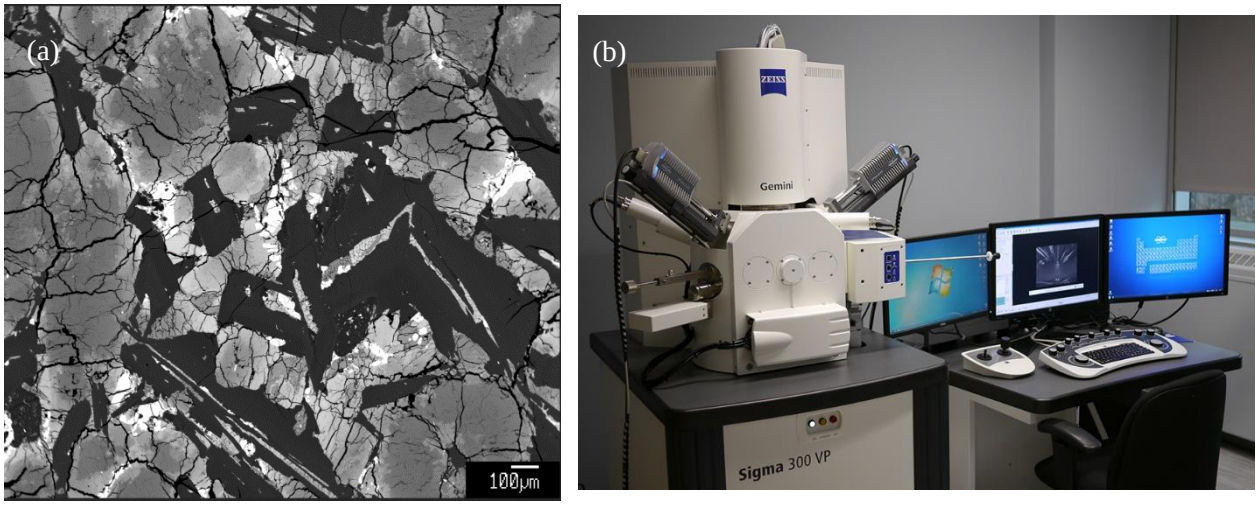

Figure S-7a *(left). A Backscattered Electron Scanning Electron Microscope image of a polished thin section of a martian basalt photo credit: Carl Agee.* ***S-7b*** *(right). An example of such an instrument is a ZEISS Sigma 300 VP*, shown here from the University of Alberta. Console and operator's table is about 2 m wide and 1 m. A couple of feet from the instrument to the wall is needed for access, <230 kg. *The naming of this reference instrument is intended for planning and discussion purposes only. Instrument-level performance requirements, sufficient to conduct a competitive procurement, have yet to be written.*

S-3.2 Confocal Raman spectrometer

A confocal Raman Spectrometer is a versatile instrument that uses a laser source to identify the molecular structure, crystallinity, and molecular interactions in inorganic and organic phases, which would be important for selecting the right sub-samples to analyze for SSAP tests and other investigations related to martian biosignatures (Table 1, goal 4). Minerals (including bound and unbound H_2O_{water}), polymorphic minerals (i.e., minerals with specific chemical compositions but different crystalline structures), and organic functional groups (including reduced carbon, PAHs, etc.) have unique Raman spectra with diagnostic Raman bands or peak positions enabling mineral phases and organic compounds identification by using available reference spectra from literature and databases (e.g., Nakamoto, 2008, Figure S-8a). A confocal Raman spectrometer uses at least one wavelength of laser to irradiate a sample at a very small spot. With a laser excitation line in the visible spectral range (approx. from 400 to 700 nm), a photon could either be elastically scattered (Rayleigh effect), i.e., scattered with no loss of energy, or inelastically scattered (Raman effect), i.e., scattered with change of energy, and consequently the Raman spectrometer observes the vibrational and rotational transitions in a crystal lattice, i.e., it is a function of molecular structure and composition. Peak positions and widths are maintained for grain sizes down to tens of nanometers (Nakomoto, 2006).

The choice of laser is dependent on the target to be examined (e.g., organic molecules with aromatic bonds are often affected by fluorescence effects, which lowers their signal-to-noise ratio). In particular, the natural luminescence of the sample may mask the Raman signal, the laser may heat and alter the sample (i.e., thermal degradation and peak broadening, or physical damage, e.g., Henry et al., 2019), or the host phase (e.g., the mineral matrix embedding fluid and/or gas inclusions) may be opaque and be absorbing at certain wavelengths. Raman signals from minerals and organic functional groups can sometimes be superimposed by competing fluorescent photons, therefore a series of different lasers are used to combat this phenomenon, especially in Earth and Planetary Sciences. Several lasers would be required on this instrument (typically 514/532, 633, 785 and 1064 nm) for inorganic and organic samples. Choosing the best illumination wavelength for a given sample is not always obvious. Many system variables must be considered to optimize a Raman spectroscopy experiment, and several of them are connected to the wavelength selection (e.g., laser power level, integration time). The nature of the sample itself guides the selection of the most appropriate laser power and wavelength to use. For instance, any absorption bands or bandgaps that may exist must be considered, and how the sample is influenced by those bands affects. Therefore, working with an unknown sample, such as Mars Sample Return samples containing potential biosignatures, it is not possible to know where to expect an absorption band, and it is possible to damage the samples (e.g., dark rock samples absorb most colors of light and are highly likely to be thermally altered or destroyed). There is little chemical element information gathered from Raman spectroscopy, so this instrument is usually used in parallel with other instruments like the FE-ESEM (section S-3.1) and/or XRF that could provide elemental chemistry. In addition, such chemical information acquired with complementary techniques could also help to select the appropriate illumination wavelength.

A Raman spectrometer, commonly using optical microscope objectives in confocal mode, can be equipped with a scanning device allowing it to display composition over a selected area of analysis, to obtain 2D and 3D compositional maps (at mm- to µm-scale). Miniaturized Raman instruments have been conceived for field investigation and planetary exploration. On the ESA/Roscosmos ExoMars 2022 rover there is a 532 nm Raman Laser Spectrometer (RLS) onboard; however, also NASA's Mars 2020 rover is equipped with laser spectrometers, within the Scanning Habitable Environments with Raman & Luminescence for Organics & Chemicals (SHERLOC) and SuperCam instruments.

Although a flat surface is ideal, no sample preparation is required for point measurements of the samples, a wide range of long working distance objective lenses would be needed for mapping, or area scans, a mapping stage with *z*-axis automatic focusing would be required, and an anti-vibration table to isolate the instrument from vibrations from the other instrumentation (Figure S-8b). Raman spectroscopy applied to geological samples could also benefit from new techniques, such as e.g., a TrueSurface module that enables confocal Raman imaging guided by surface topography. 3D chemical characterization on samples can be carried out precisely along or at a set distance from a surface without requiring sample preparation. The instrument shown uses a Class 3B laser, and hence should be placed either in a separate room, or with the ability to separate it from the other instruments (by optical curtain, for example).

(a)

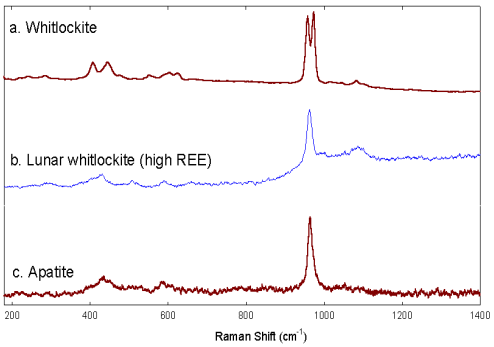

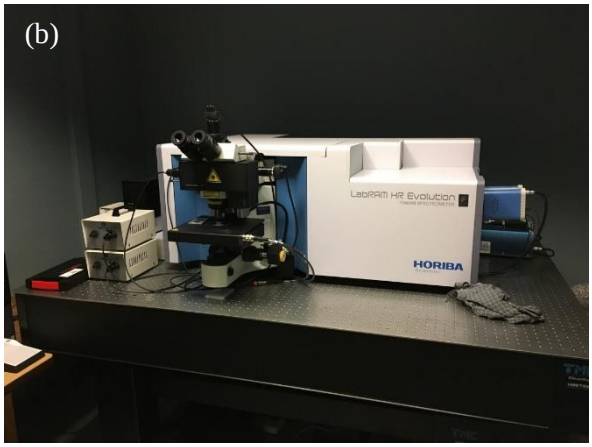

Figure S-8a *(left): An example of Raman spectra of phosphates minerals within Zagami (a martian meteorite) and a lunar rock from: http://epsc.wustl.edu/haskin-group/Raman/zagami.htm* ***S-8b*** *(right). A HORIBA LabRAM HR* Raman Spectrometer, shown here from the Smithsonian, (W x H x D) ~127 cm x 64 cm x 64 cm, benchtop system <91 kg with a class 3B Laser. *The naming of this reference instrument is intended for planning and discussion purposes only. Instrument-level performance requirements, sufficient to conduct a competitive procurement, have yet to be written.*

S-3.3 Deep UV fluorescence microscopy

Deep UV Fluorescence is non-destructive technique for mapping the distribution of organic compounds, which would be important for selecting the right sub-samples to analyze for SSAP tests and other investigations related to martian biosignatures. Most organic and many inorganic materials absorb strongly in the deep UV range from about 220 nm to 300 nm (Abbey et al., 2017, Figure S-9). Each compound has a unique excitation-emission fingerprint that can be used to identify the compound and provide information about the material (Table 1 goal 4). The most common deep Ultraviolet (UV) lasers emit at 248.6 and 224.3 nm and are typically used for searching for organics, a major goal of the MSR campaign Figure 19). Although some of the setup of a UV fluorescence spectrometer is like a Raman spectrometer, the NIR/Visible Raman systems focus on high resolution “micro”-mapping. This is necessary to optimize the spectral quality, however it is not an ideal approach to search for organics over centimeter areas – i.e., using a 1 µm beam to scan a sample is very time consuming. Comparatively, the deep UV spectroscopy systems are best at enabling mapping on multiple spatial scales. Commercially available instruments do not integrate the wavelengths in a manner that is effective for multi-wavelength analysis of a geologic sample where both organics and mineral analysis over multiple scales is necessary (*Pers. Comm.* Bhartia, 2020; Figure S-20) so future work should be done to make sure a proper analytical system is in place for the samples when they are returned (See Section 8.1 Future Work 13).

On the Mars2020 rover there is an arm-mounted deep UV (DUV) resonance Raman and Fluorescence spectrometer called the Scanning Habitable Environments with Raman & Luminescence for Organics & Chemicals (SHERLOC). It utilizes a 248.6 nm DUV laser and <100-micron spot size with a spatial resolution of 30 microns (Bhartia et al., 2021). The samples collected on Mars should have SHERLOC information included in the sample dossier, so comparing this information would be very useful for the sample catalog.

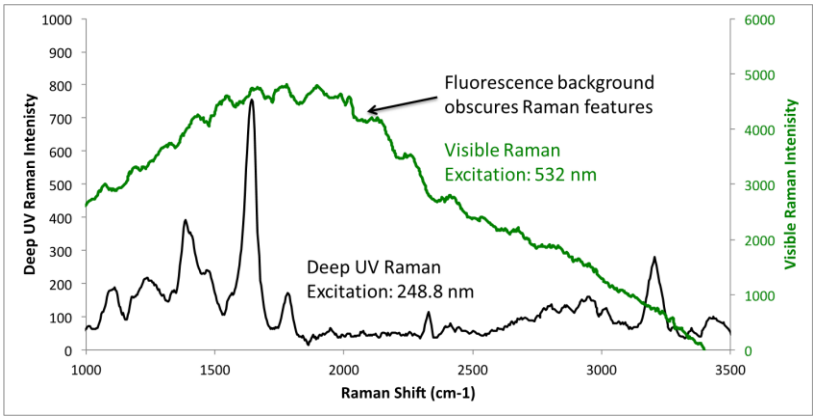

Figure S-19. *Deep UV Raman spectrum using a 248.8 nm laser compared to one obtained with a 532 nm laser. Photo credit: Photon Systems Inc.*

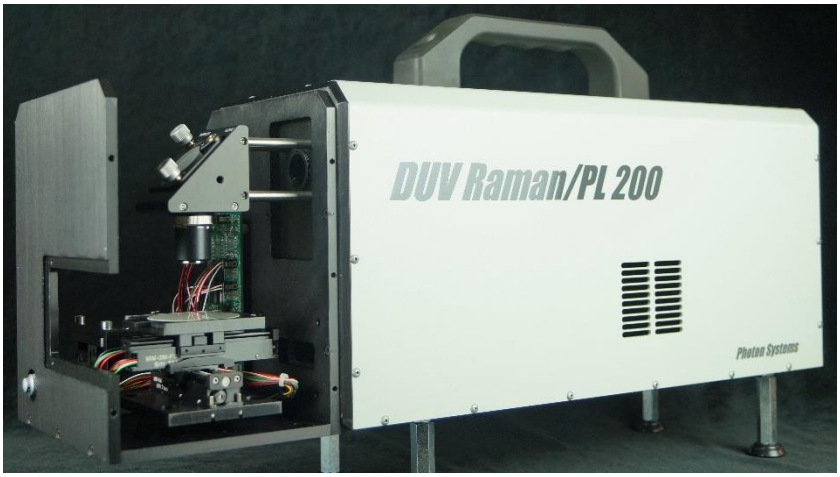

Figure S-20. *An example of a Deep UV system, from Photon Systems Inc. DUV PL 200*, (W x H x D) 18 cm x 20 cm x 61 cm, benchtop system, <11 kg, can be vibration sensitive and has a class 3B laser. *The naming of this reference instrument is intended for planning and discussion purposes only. Instrument-level performance requirements, sufficient to conduct a competitive procurement, have yet to be written.*

S-3.4 Fourier transform infrared spectrometer

Fourier Transform Infrared Spectroscopy is a destructive technique that identifies anion functional groups (such as SiO_2, CO_3, PO_4 and SO_4) and characterizes how water is physically and chemically bound to mineral phases, which is critical in describing several inorganic phases, such as carbonates.

When infrared radiation is passed through a sample, some radiation is absorbed by the sample, and some is transmitted. The resulting signal at the detector is a spectrum representing a molecular 'fingerprint' of the sample, which can be matched against spectral databases. Different chemical structures (molecules and compounds) produce different spectra due to their responses (vibrations, stretches, etc.) to IR

radiation and FTIR thus provides complementary information and potential for molecular bond interpretation (Table 1, goal 4) to elemental analysis methods such as XRF (Anderson et al., 2005) and Raman spectroscopy.

One of the advantages of FTIR is that it provides information on both inorganic minerals and organic compounds. FTIR is not hampered by laser damage or fluorescence that can occur in such techniques as Raman spectroscopy. Fundamental vibration modes of anion functional groups such as SiO_2, CO_3, PO_4 and SO_4 are found in the mid-infrared region of 4000–500 wave numbers. The infrared bands are diagnostic and exhibit measurable band shifts with cation substitution that provide for mineral identification (Socrates, 1980; Anderson et al., 2005).

For the radiation to transmit through the sample, a small amount of material must be ground using a dry mortar and pestle, mixed with potassium bromide (KBr), and pressed into a pellet or a thin section prepared. The powder method is destructive to the sample, but typically no more than several milligrams is needed. FTIR detects a wide range of organic compounds and can give information about organic-mineral relationships (Figure S-21a) (Benning et al., 2004). The infrared analysis experiment does not target particular molecules but readily detects numerous classes of molecules. FTIR is complementary to Raman spectroscopy, but is not hindered by fluorescence issues and provides better sensitivity for many minor components (Marshall and Marshall, 2015). FTIR provides particularly sensitive measure as to the amount of water in a mineral sample and how this water is physically and/or chemically bound to the mineral. Information collected is complementary to several other instruments, including Deep UV Fluorescence, and gas chromatography. Considering instrumental modification, such as Attenuated Total Reflection (ATR) and Diffuse Reflectance Infrared Fourier Transform Spectroscopy Analysis (DRIFT) reduces sample preparation requirements and enables diverse analytical strategies (Figure S-21b).

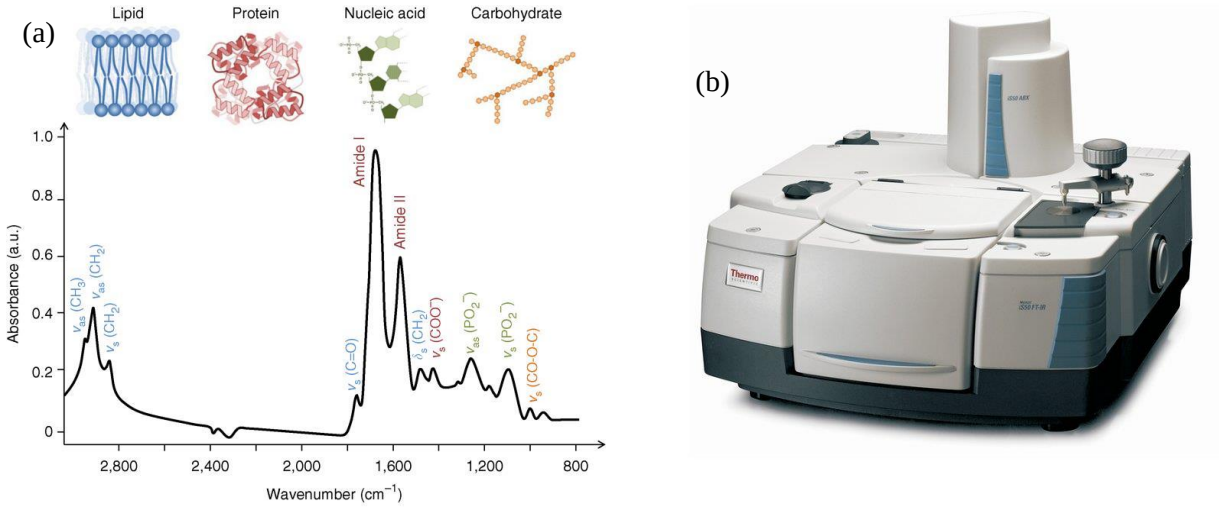

Figure S-21a *(left). Using Fourier transform IR spectroscopy to analyze biological materials (Baker et al., 2014);* ***S-21b****. An example of a FTIR system, ThermoScientific Nicolet™ iS50 FTIR Spectrometer* benchtop system, (W x H x D) 64 cm x 71 cm x 69 cm, approx. 63 kg. *The naming of this reference instrument is intended for planning and discussion purposes only. Instrument-level performance requirements, sufficient to conduct a competitive procurement, have yet to be written.*

S-3.5 *Micro X-ray diffractometer*

X-ray diffraction is a non-destructive technique (in itself – albeit the sample preparation) for identifying the phase and the degree of crystallinity of primary and secondary phases in samples. This technique is especially useful for hydrated phases and carbon-bearing phases that need to be identified quickly and in real time for time sensitive measurements.

Crystalline solids have a long-range repeating structure which corresponds to a microscopic arrangement of atoms that is repeated periodically and interacts with infalling X-rays. X-rays are generated in a cathode ray tube by heating a filament to produce electrons, which are accelerated toward a target by applying a voltage and then bombarding the target material with electrons. When electrons have enough energy to dislodge inner shell electrons, characteristic X-ray spectra are produced. When the geometry of the incident X-rays impinging the sample satisfies the Bragg Equation, constructive interference occurs and a peak in intensity occurs; this intensity is measured by a detector and processes this X-ray signal and converts the signal to a count rate which is then outputted. Progress in X-ray focusing technologies combined with efficient vibration damping systems allow today for an X-ray beam in the order of a few tens of nanometers in size, but more routinely in a micrometer size range (Tamura and Kunz, 2015). Peak intensity, peak position, and peak broadness are all ways to evaluate mineral abundances and the crystallinity of the sample and are compared to databases of known mineral diffraction patterns for identification of phases (Table 1 goal 4). If the sample is amorphous (i.e., lacks long-range repeating atomic structure), there will be no sharp diffraction peaks in the diffraction pattern, but other important information can be gained. For example, there will be X-ray scattering which provides constraints on local (i.e., short-range) structure. The nature of nominally X-ray amorphous or poorly crystalline samples can be constrained with a total scattering experiment that analyses data using a pair distribution function to determine constraints on next neighbor relationships and adjacent structural environments. This experiment can be performed with a laboratory diffractometer but requires a higher energy X-ray source than typically used (e.g., Ag source) and a suitable detector (Figure S-22).

Figure S-22*. An example of a Malvern Panalytical Empyrean powder X-ray diffractometer, Weight: 1400 kg, Exterior dimensions: 195 x 116 x 140 cm (full system). *The naming of this reference instrument is intended for planning and discussion purposes only. Instrument-level performance requirements, sufficient to conduct a competitive procurement, have yet to be written.*

Samples can be prepared into a powder (e.g., using a dry mortar and pestle) to maximize the amount of incident X-rays interacting with the sample, or individual grains can be examined *in situ* with little or no sample preparation (Flemming, 2006; Figure S-23a). Ideally the samples would have a flat surface so the incident X-rays can interact with the sample without surface roughness getting in the way.

X-ray diffraction has some advantages over other techniques. It has been used widely in Earth Sciences, so the database of minerals is quite comprehensive, and many studies have been performed on similar materials. X-ray diffraction provides structural information, but not chemical information (which can be inferred from cell parameters and peak positions) but typically is used in conjunction with an instrument that can measure chemistry such as an FE-SEM-EDS or -WDS, or XRF.

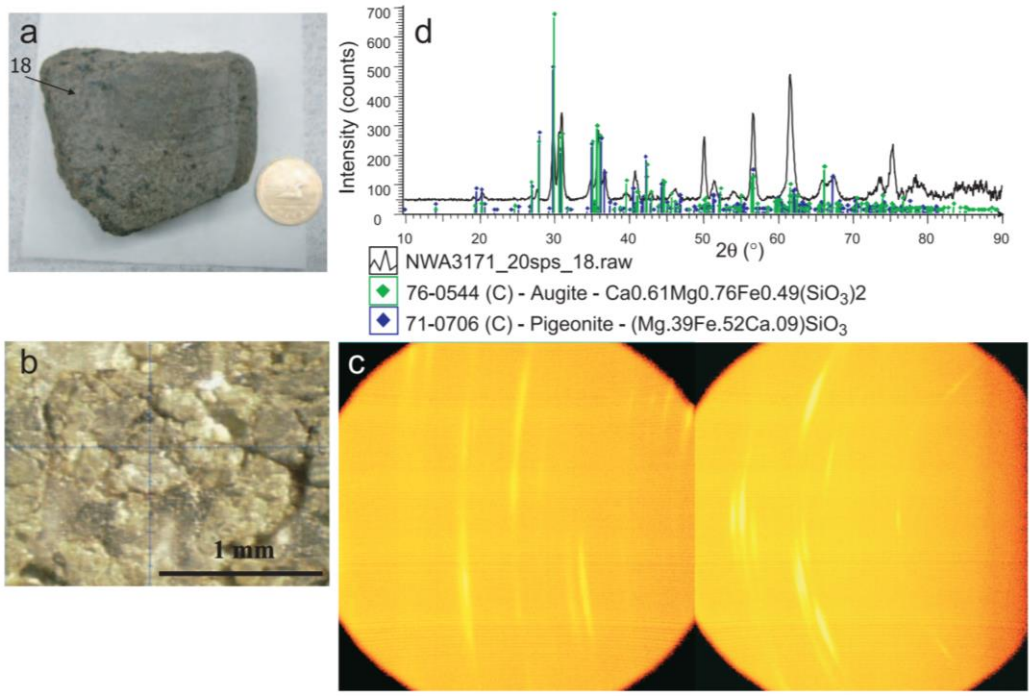

Figure S-23a*. Micro X-ray diffractometer data from martian meteorite NWA 3171. (**S-23a**) Main mass of NWA 3171 showing location of X-ray analysis of spot 18 on cut surface; (**S-23b**) Image of spot 18 as it appeared under the optical microscope monitor on the micro diffractometer (maximum magnification); (**S-23c**) GADDS (General Area Diffraction Detector) images from spot 18 showing streaked diffraction lines, attributed to strain (coupled scan, 3 frames, 24 min per frame, 500 µm beam); (**S-23d**) Plot of intensity versus 2ϑ for spot 18 (after background subtraction) showing a good match with two clinopyroxenes: augite (e.g., 76–544) and pigeonite (e.g., 71–706) (From Flemming, 2006).*

S-3.6 Energy dispersive X-ray fluorescence spectrometer

Energy Dispersive X-ray fluorescence (XRF) is a non-destructive, bulk surface technique to determine the chemical elements present in the specimen which is required for sample allocation purposes where phase identification and chemistry is required (Table 1 goal 4 “bulk chemistry”). These measurements are complementary to XRD, SEM and Raman Spectroscopy. When a primary X-ray is absorbed by the atom by transferring all its energy to an innermost electron this is called the photoelectric effect. During this process, if the primary X-ray has sufficient energy, electrons are ejected from the inner shells creating vacancies. These vacancies present an unstable condition for the atom, and another electron transfers from the outer shells to the inner shells which gives off a characteristic X-ray photon whose energy is the

difference between the two binding energies of the corresponding shells (Figure S-24). Since each element has a unique set of energy levels, each element produces X-rays at a unique set of energies allowing one to non-destructively measure the elemental composition of a sample.

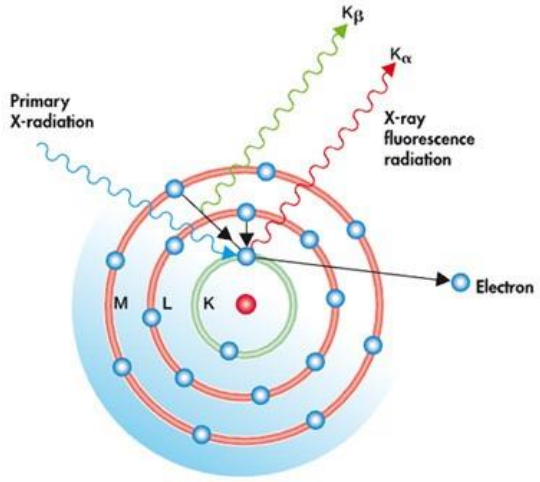

Figure S-24*. Atomic model for the X-Ray Fluorescence Analysis method. When the primary radiation interacts with the element, a generated inner vacancy is filled with an external bound-electron and the excess of energy is released (photon emission). The energy of generated X-ray photon (fluorescence) is determined by the energy of the involved electronic levels (see K_α and K_β lines in the figure) which in turn depends on the nucleus characteristics. From: X-rays produced with https://wpo-altertechnology.com/xrf-x-ray-fluorescence-spectroscopy-hi-rel-parts/*

XRF provides quantitative bulk chemical analyses of the main elements and trace elements (in abundances >1 ppm) present in the specimen (Figure S-25a). Instrumentation is improving, but low Z (atomic number) elements are more difficult to measure, and therefore we suggest the application of a low element detector that can measure C, N, O with at least a 300-micron spot size. Although a flat surface is better, no sample preparation is required. Benchtop instruments are closed X-ray source instruments, with full X-ray shielding (Figure S-25b).

On the Mars 2020 rover's robotic arm there is an instrument for X-ray lithochemistry called PIXL, which is a micro-focus X-ray fluorescence instrument (Allwood et al., 2020). PIXL will be able to scan a 0.12 mm-diameter X-ray beam across a 25 x 25 mm target area, measuring the abundance and distribution of elements with high spatial resolution, sensitivity, and accuracy (Allwood et al., 2020). It is worth noting that the PIXL data is from very small spots of material near where the sample is ultimately collected but not on the sample itself (because it is drilled from the subsurface). For that reason, it is a high priority to generate data from the sample to link back to PIXL data. The abundances and distribution of elements at submillimeter scales should be included in the sample dossier for every tube, so having an instrument with similar capabilities in the PE instrument suite would be potentially advantageous.

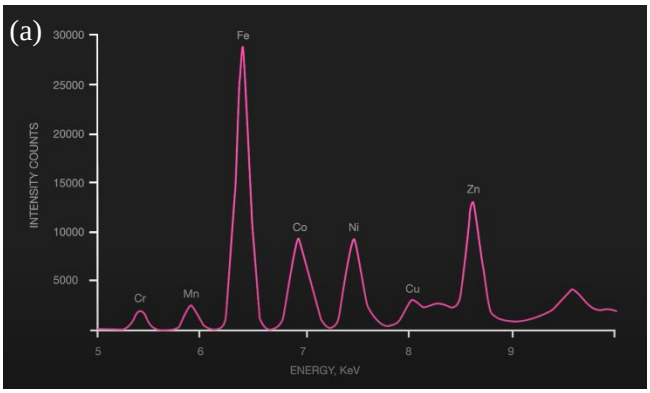

Figure S-25a *(left). Example of an X-ray fluorescence spectra, from: https://wpo-altertechnology.com/xrf-x-ray-fluorescence-spectroscopy-hi-rel-parts/* ***S-25b*** *(right). Bruker S2 Puma* with light element detector and mapping stage, Weight: 132 kg, Exterior dimensions: (W x D x H) 67 cm x 71 cm x 57 cm from: https://www.s2puma.com/images/s2-puma/PDF/S2_PUMA_Brochure_DOC-B80-EXS015_V2_high.pdf . *The naming of this reference instrument is intended for planning and discussion purposes only. Instrument-level performance requirements, sufficient to conduct a competitive procurement, have yet to be written.*

S-3.7 Petrographic and stereo microscopes

Petrographic and stereo microscopes are required to observe samples with visible light to allow for the study of minerals, mineral textures, mineral habits, and degree of crystallinity in a mineral phase (Figure S-26a) to select the appropriate samples for sample allocation. Although destructive in preparation, thin sections would be required by PIs for experiments (Table 1 goals 1–3 and details). Observations require several objective lenses (2x–100x), with a rotation stage, analyzer, and a polarizer; polarized reflected light might be considered as well. The microscopes will need imaging software, and a computer with high-end video cameras for observations (and remote observations). These microscopes must have photographic cameras and video camera capabilities so that material can be completely visually recorded for the sample catalog (Figure S-26b). Microscopic cameras can also be adapted for use as a petrographic microscope for polarized transmitted or reflected light imaging of any produced thin or thick sections.

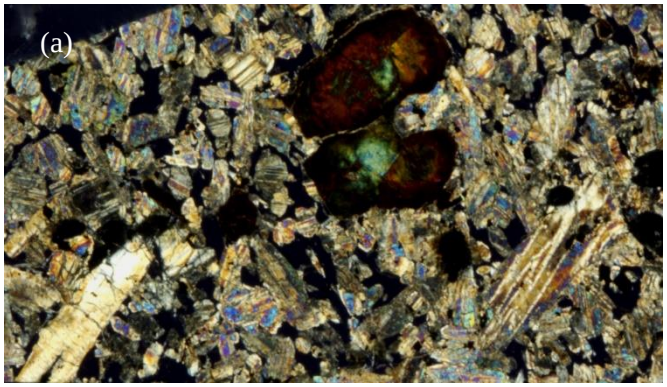

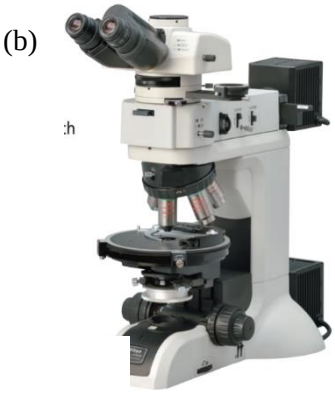

Figure S-26a *(left). Example of a petrographic thin section image (width 5 mm) in cross-polarized light of martian meteorite NWA 2046 https://www2.jpl.nasa.gov/snc/nwa2046.html;* ***S-26b*** *(right). An example of a tabletop sized Nikon ECLIPSE LV100N POL* petrographic microscope, (W x H x D) ~51 cm x 71 cm x 64 cm, ~18 kg. *The naming of this reference instrument is intended for planning and discussion purposes only. Instrument-level performance requirements, sufficient to conduct a competitive procurement, have yet to be written.*

S-4. Sample Processing

S-4.1 Microparticle processing

S-4.1.1 Micromanipulator

Motorized micromanipulators are used to manipulate small objects or specimens under a microscope. A benefit to using motorized micromanipulators is the precision movement on a variety of axes that enables absolute manipulation far superior to traditional manual manipulation. Common actions including holding or cutting are often controlled via joystick (Figure S-27). The Astromaterials Acquisition and Curation office at NASA's Johnson Space Center, as part of the Advanced Curation program, has been working on developing micromanipulators for sample curation beyond the 3-axis. The Meca500, e.g., is a six-axis robotic arm with a range of motion reaching 260 mm, enabling it to enhance micromanipulation within glovebox operations (Cowden et al., 2019) and should be investigated further for the SRF (See Section 8.1 Future Work 14).

Figure S-27*. Example a 3-axis micromanipulator from AxisPro from MicroSupport.*

** The naming of this reference instrument is intended for planning and discussion purposes only. Instrument-level performance requirements, sufficient to conduct a competitive procurement, have yet to be written.*

S-4.1.2 Ultramicrotome

An ultramicrotome (Figure S-28) prepares ultra-thin sections of materials from 1 µm to 15 µm thickness, as well as the perfectly smooth surfaces required for Light Microscopy, Transmission Electron Microscopy, SEM, and Atomic Force Microscopy examination if required for the science investigations.

Figure S-28*. Example of a ultramicrotome: LEICA UC7 ultramicrotome*.*

** The naming of this reference instrument is intended for planning and discussion purposes only. Instrument-level performance requirements, sufficient to conduct a competitive procurement, have yet to be written.*

S-4.2 Macrosample processing

S-4.2.1 Dry wire saw

A dry wire saw would be used to cut and section the samples. Included in this report is an example of a dry wire saw that could be used for these purposes, a Wells 3500P wire saw (Figure S-29). The saw can be fitted with a USB/Wi-Fi 10x to 140x microscope to accurately visualize the cutting point, which should be included for interactions with the PIs and for documentation of the cutting. Note the cutting could occur within an isolator or outside of the isolator as required.

***Figure S-29**. Example of a dry wire saw: Wells 3500P**

W x W x H: 410 mm x 345 mm x 460 mm Weight: 13.8 kg.

**The naming of this reference instrument is intended for planning and discussion purposes only. Instrument-level performance requirements, sufficient to conduct a competitive procurement, have yet to be written.*

S-4.2.2 Grinding and polishing equipment

Having the ability to prepare sub-samples for the scientific community is an important function of the PE stage. The polishing and grinding facilities need to be manual or semi-manual with the size and the precious nature of the samples and one example of that is the Struers LaboSystem (Figure S-30). There are ongoing costs associated with this instrumentation, such as adhesive discs, suspensions, lubricants, films and cloths and likely other instruments that will be required, like an ultrasonicator to support the polishing and grinding needs, but this will need to be looked at in future working groups.

***Figure S-30**. Example of a grinding and polishing setup: Struers LaboSystem**.*

** This naming of this reference instrument is intended for planning and discussion purposes only. Instrument-level performance requirements, sufficient to conduct a competitive procurement, have yet to be written.*

S-4.2.3 Carbon and/or gold coater

For sample preparation for the FE-SEM Microscope, a sputter coater would be required (Figure S-31). Ideally the instrument would be able to deposit thin layers of both carbon and gold on the prepared sample, to reduce surficial charging in the FE-SEM. The instrument should not heat the sample and be able to rapidly coat the sample.

Figure S-31*. Example of a carbon coater: SPI Module Sputter Coater with pump**

W x D x H: 220 mm x 325 mm x 200 mm Weight: 10.2 kg.

**This naming of this reference instrument is intended for planning and discussion purposes only. Instrument-level performance requirements, sufficient to conduct a competitive procurement, have yet to be written.*

S-5. Overview of Analytical Instruments That Were Considered, but Ultimately Not Included

S-5.1 Synchrotron light sources

Synchrotron light sources offer an array of powerful non-destructive characterization techniques that could be applied to the Mars returned samples. These would include hard X-ray (>5 keV) and tender X-ray (1–5 keV) microprobes, micro- and nano-X-ray Fluorescence (XRF), X-ray Absorption Spectroscopy (XAS) and XRD techniques in both 2D and 3D (tomography). The X-ray energies (~160–450 keV) and fluxes associated with X-ray Computed Tomography scanner (XCT) are considered less damaging to organics than low-energy X-rays (~8–22 keV) and fluxes that are available with monochromatic X-ray sources at Synchrotron facilities (Moini et al., 2014; Bertrand et al., 2015; Friedrich et al., 2016; 2019; Hanna and Ketcham, 2017). These techniques can be used to quantify major and trace element compositions, identify mineral phases, determine oxidation-reduction states, and detect biomarkers. Additionally, synchrotron science has benefited from decades of experience in meeting the challenges in preparation, handling, and containment of terrestrial materials for analysis, including measurements on atmospheric particles, deep-sea samples, and other exotic terrestrial environments. However, due to the need to send the samples out of the SRF, clear or sterilize them or store them in containers that keep them in biocontainment, these techniques would be most appropriate in the SRF through the Pre-BC, BC, and PE sequence. Therefore, use of synchrotron light sources should not be included in the curation function of the SRF. Instead, it is recommended that future planning should explore how best to maximize Mars sample science (post-PE) through synchrotron light sources. Considerations include requirements for measurements on pristine samples, but also logistics including packaging, shipping, handling, and biocontainment that would include biohazard security and preservation. Although synchrotron-based XCT labs can also achieve the same high energy X-ray energies that is standard in lab-based XCT instruments, the Curation Focus Group determined that lab-based XCT was sufficient and should be implemented within the SRF.

S-5.2 Penetrative X-ray Raman spectroscopy (XRS) for Pre-BC

In section S-1.2, the merits of penetrative imaging using a X-ray Computed Tomography scanner (XCT) for Pre-BC are discussed. Here we consider penetrative X-ray Raman Spectroscopy (XRS) which is a non-resonant inelastic X-ray scattering from core electrons and can be used to study low-Z element electronic structure using high-energy X-rays. This technique could be considered for applying high energy photons to probe low energy absorption edges, and potentially search for organic species (especially carbon-rich compounds) in the Mars returned samples while they are still contained in the sealed titanium sample tubes, as part of curation in Pre-BC. Unfortunately, this is not a viable option for several reasons: 1) the concentration of organic species, for example, possible bacterial cells in martian soil, would be very small, so the signal would be extremely weak; 2) the measurement would be done in tomographic mode, hence the signal would be even weaker from required small image voxels; 3) there would be high background noise of carbon from atmospheric CO_2, adsorbed carbon surface species, and potential carbon contamination in beamline optics and filters - any presence of inorganic carbon would further complicate detecting organic carbon; 4) at the high energies required (>40 keV), the energy resolution or interpretation of carbon X-ray absorption near edge structure (XANES) would be challenging to achieve; 5) detecting organic sulfur species would be marginally easier than carbon, but would still face the same difficulties, and would be closer to the interferences from high-concentration silicon and aluminum which are likely to be present in the Mars returned samples; 6) the radiation dose required to achieve a measurable signal would damage the sample. This damage would be through direct radiation damage, but also by the creation of radicals, and the damaging effects of intense secondary fluorescence by heavier metals, in particular iron and titanium, in the Mars returned sample and tube.

S-5.3 Neutron Computed Tomography

Neutron Computed Tomography (NCT) would need to be done outside of the SRF, so a BSL-4 containment sample holder would need to be designed to contain the sample tube to be transported to a Neutron Facility. This sample holder would need to be designed in such a way that it would be neutron transparent. Even with that, there are concerns that these measurements can be detrimental to organics and other properties of the samples. Also, it has been shown that neutron capture during NCT alters some isotope ratios (Treiman et al., 2018). Furthermore, titanium has a large macroscopic neutron absorption cross section, which efficiently shields (i.e., attenuate through absorption) neutrons, which may impede measurements of samples in the unopened Ti tubes that house Mars sample cores. For these reasons, we have removed this as an option for a viable instrument for pre-BC.

S-5.4 Nuclear magnetic resonance (NMR)

Double- and single-resonance solid-state (^{1}H and ^{13}C) nuclear magnetic resonance (NMR) measurements for organic compounds were discussed by the Curation Focus Group and although extremely interesting and worthwhile measurements, we felt this instrument is out of the remit of the initial sample characterization goals for Curation, and more for the objective-driven investigations and opportunity-driven investigations; therefore, this instrument was not included in the SRF but could be included if required for the science teams.

S-5.5 Mass spectrometers

There was some discussion by the Curation Focus Group on the need for a series of Mass Spectrometers for curation purposes. In the end, although some overlap with the curation goals, these instruments are more relevant to time-sensitive measurements, particularly for the analysis of headspace gases and tube sealing (Tosca et al., 2022) and are therefore not discussed here.

References

Abbey W. J., Bhartia R., Beegle L. W., *et al.* (2017) Deep UV Raman spectroscopy for planetary exploration: The search for in situ organics. *Icarus*, 290: 201-214.

Allwood A. C., Wade L. A., Foote M.C., *et al.* (2020) PIXL: Planetary instrument for X-ray lithochemistry. *Space Sci Rev* 216: 134.

Anderson M. S., Andringa J. M., Carlson R. W., and others. (2005) Fourier transform infrared spectroscopy for Mars science. *Review of Scientific Instruments*, 76.

Benning L. G., Phoenix V. R., Yee N., and Konhauser K. O. (2004) The dynamics of cyanobacterial silicification: An infrared micro-spectroscopic investigation. *Geochimica Et Cosmochimica Acta*, 68: 743-757.

Bertrand L., Schoder S., Anglos D., *et al.* (2015) Mitigation strategies for radiation damage in the analysis of ancient materials. *Trac-Trends in Analytical Chemistry*, 66: 128-145.

Bhartia R., Beegle L.W., DeFlores L. *et al.* (2021) Perseverance's Scanning Habitable Environments with Raman and Luminescence for Organics and Chemicals (SHERLOC) Investigation. *Space Sci Rev* 217: 58.

Carlson W. D. (2006) Three-dimensional imaging of earth and planetary materials. *Earth and Planetary Science Letters*, 249: 133-147.

Cowden, T. R., Snead, C. J., Jang, J. H., *et al.* (2019) Meca500 Robotic Arm Developments Towards Astromaterials Curation Applications. In *82nd Annual Meeting of The Meteoritical Society, Sapporo, Japan*, (LPI Contribution No. 2157).

Flemming R. (2006) Micro X-ray diffraction (μXRD) a versatile technique for characterization of Earth and planetary materials. *Canadian Journal of Earth Sciences,* 44(9): 1333–1346.

Friedrich J. M., Glavin D. P., Rivers M. L., and Dworkin J. P. (2016) Effect of a synchrotron X-ray microtomography imaging experiment on the amino acid content of a CM chondrite. *Meteoritics & Planetary Science*, 51: 429-437.

Friedrich J. M., McLain H. L., Dworkin J. P., *et al.* (2019) Effect of polychromatic X-ray microtomography imaging on the amino acid content of the Murchison CM chondrite. *Meteoritics & Planetary Science*, 54: 220-228.

Hanna R.D. and Ketcham R.A. (2017) X-ray computed tomography of planetary materials: A primer and review of recent studies. *Geochemistry, 27*(4):547–572.

Henry D. G., Jarvis I., Gillmore G., and Stephenson M. (2019) Raman spectroscopy as a tool to determine the thermal maturity of organic matter: Application to sedimentary, metamorphic and structural geology. *Earth-Science Reviews*, 198.

Lepaulard C., Gattacceca J., Uehara M., *et al* (2019). A survey of the natural remanent magnetization and magnetic susceptibility of Apollo whole rocks. *Physics of the Earth and Planetary Interiors, 290*:36–43.

Marshall A.O. and Marshall C.P. (2015). Vibrational spectroscopy of fossils. *Palaeontology, 58*(2), 201–211.

McCubbin F. M., Shearer C. K., Barnes J. J., *et al.* (2021) The ANGSA Program: A low-cost lunar "sample return mission". An overview and progress over the last 18 months. *In 52nd Lunar and Planetary Science Conference, held virtually* (LPI Contribution No. 2548).

Moini M., Rollman C. M., and Bertrand L., (2014) Assessing the impact of synchrotron X-ray irradiation on proteinaceous specimens at macro and molecular levels. *Analytical Chemistry 86*:9417–9422.

Nagendran R., Thirumurugan N., Chinnasamy N., Janawadkar, *et al* (2011) Development of high field SQUID magnetometer for magnetization studies up to 7 T and temperatures in the range from 4.2 to 300 K. *Review of Scientific Instruments,* 82.

Nakamoto K. (2008) Theory of normal vibrations. In *Infrared and Raman spectra of inorganic and coordination compounds: Part A*: *Theory and Applications in Inorganic Chemistry*, edited by K. Nakamoto, 6th edition, pp 1–147.

Socrates G. (1980) *Infrared and Raman Characteristic Group Frequencies: Tables and Charts, 3rd Edition*. Wiley. 366 pp.

Sun L., Lucey P. G., Flom A., *et al* (2021) Multispectral imaging and hyperspectral scanning of the first dissection of core 73002: Preliminary Results. *Meteoritics and Planetary Science*, 56: 1574-1584.

Tamura N. and Kunz M. (2015) A concise synchrotron X-ray microdiffraction field guide for the Earth scientists. *Boletín de la Sociedad Geológica Mexicana, 67*(3):467–478.

Tosca N. J., Agee C. B. ,Cockell C. S., et al. (2022) *Time-sensitive aspects of Mars Sample Return (MSR) Science. Astrobiology*, 22.

Treiman A. H., LaManna J. M., Anovitz L. M., *et al* (2018) Neutron computed tomography of meteorites: Detecting hydrogen-bearing materials. In *49th Lunar and Planetary Science Conference*, The Woodlands, Texas, (LPI Contrib. No. 2083).

Uehara M., Gattacceca J., Quesnel Y., *et al.* (2017). A spinner magnetometer for large Apollo lunar samples. *Review of Scientific Instruments 88*.

Welzenbach, L. C., Fries, M. D., Grady, M. M., *et al.* (2018) Mars sample return processing: X-Ray Computed Tomography of the Mars 2020 cache. In *European Planetary Science Congress 2018*, Berlin, Germany, Abstracts Vol. 12, EPSC2018-1182.

Zeigler R. A., Hanna R., Edey D., et al. (2021) Using X-ray Computed Tomography to image Apollo Drive Tube 73002. In *52nd Lunar and Planetary Science Conference, held virtually* (LPI Contribution No. 2548).